VII Brazilian Symposium on Rock Mechanics – SBMR 2016
Rock Mechanics and Rock Engineering for Innovation and Development
ISRM Specialized Conference 19-22 October, Belo Horizonte, Minas Gerais, Brazil

Integrating Terrestrial Laser Scanning and Discrete Fracture Network Approaches for Tunnel Modelling in Fractured Rock Masses

Pedro Pazzoto Cacciari
University of São Paulo, São Paulo, Brazil. ppazzoto@gmail.com.br

Marcos Massao Futai
University of São Paulo, São Paulo, Brazil. futai@usp.br
Academic visitor at University of Cambridge, Cambridge, UK.

SUMMARY: This article presents a methodology for creating 3DEC block models of tunnels constructed in fractured (blocky) rock masses, based on the Terrestrial Laser Scanning technique (TLS) and Discrete Fracture Networks (DFN). Several aspects of discontinuity mapping using TLS, discontinuity analyses by window-sampling methods and DFN modeling are discussed. The Monte Seco tunnel (Vitória-Minas Railway), located in the State of Espirito Santo (Brazil), is used as an example. Three discontinuity sets (two fractures sets, F1 and F2, and the rock foliation, Sn) were mapped (with TLS) and analyzed to obtain the probability distributions of the discontinuity diameters and orientations. Next, the volumetric intensities (P32) were calculated and DFNs were generated to create the 3DEC block model of an 8 m long section of this tunnel.

KEYWORDS: Discontinuity, Terrestrial Laser Scanner, Discrete Fracture Network, Tunnel.

1 INTRODUCTION

Several old tunnels in Brazilian roads and railways were constructed in hard rock masses without any support system. Recently, some of these tunnels are presenting localized problems of rock falls mainly related with rock discontinuities distributions and some punctual weathering processes. The Vitoria-Minas Railway (VMR), owned by VALE SA, is one of the oldest railways in Brazil and has about twenty tunnels in this condition, requiring geological and geotechnical investigations to provide parameters and evaluate the stability state. Considering this problem, a partnership between Escola Politécnica of the University of São Paulo and VALE SA was initiated to propose a methodology and study of these tunnels. The lengths of these tunnels vary from hundreds of meters to a few kilometers, which makes conventional field discontinuity mapping a strenuous and time-consuming task since considerable detail is required. In addition, it is difficult to obtain the actual position and geometrical parameters (generally described as orientation, frequency and size) of all the discontinuities in tunnels with the conventional geological mapping, mainly in the higher regions of the tunnel section.

This paper presents an approach to tunnel modelling in fracture rock masses using discontinuity mapping obtained from terrestrial laser scanning (TLS) images and discrete fracture networks (DFN) generations. The large volume of discontinuity data obtained by terrestrial laser scanner allows applying several sophisticated discontinuity analyses (orientation, length and frequency), and defining the volumetric intensity of each discontinuity set along the tunnel. Thus, representative and reliable 3DEC block models of the tunnel can be created for different tunnel positions. Moreover, since the mechanical characterization of the rock mass is also properly made, the present approach can be a powerfull tool for stability analyses in Rock Mechanics. Especially for reassessing old uncovered tunnels, as there are several in VMR, in which the rock face can be completely used for discontinuity mapping.

2 METHODOLOGY

The faro focus 3D laser scanner was used to generate the tunnel point cloud (Figure 1) and the Polyworks software (InnovMetric Software) was used to perform the discontinuity mapping. The discontinuity analyses were performed in Visual Basic-Excel programs and both the discrete fracture networks and 3D block model were generated in 3DEC software (Itasca Consulting Group). The methodology can be summarized by the following steps:

1) Full discontinuity mapping of the TLS point clouds measuring all discontinuity positions, trace lengths, and orientations.

2) Discontinuity analysis for determining the probability density functions (*pdf*) of the diameters and orientations of each discontinuity set.

3) Using a 3DEC-Fish code to calculate the volumetric intensities (P32) of each discontinuity set and use these values as stopping criteria for DFN generations.

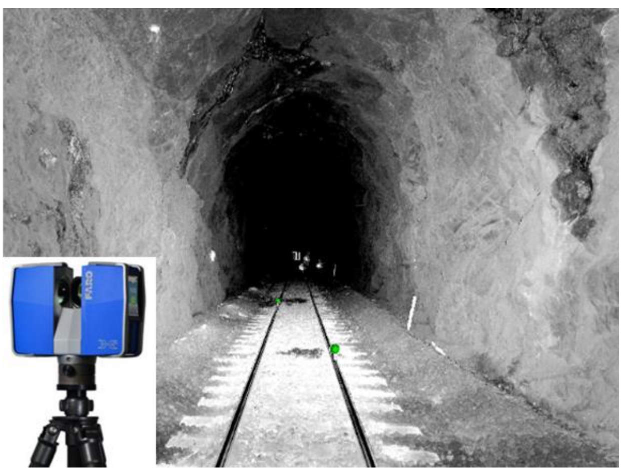

Figure 1. Faro Focus 3D Laser Scanner (Faro Inc.) and an example of the TLS tunnel image (point cloud) generated by this instrument.

2.1 Discontinuity mapping in the TLS.

The discontinuity mapping in TLS point cloud consists basically in interpreting the discontinuities apparent in the tunnel rock face and taking measurements. The orientation is measured by selecting coplanar points of the discontinuity exposed areas and extracting the normal vector of a plane fitted in these points. Next, all the normal vectors measured are converted into the structural geology notation (Dip/Dip direction). Discontinuity traces are intersection between discontinuities and the rock face. The trace lengths are measured by taking the distance between the endpoints of polylines fitted in these traces. Figure 2 shows examples of trace lengths and orientation measurements in the point cloud.

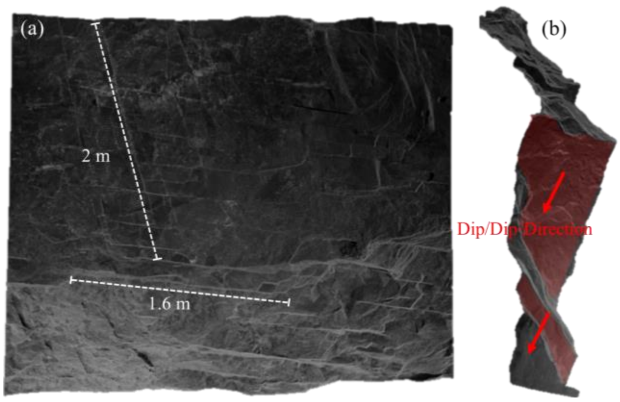

Figure 2. Discontinuity measurements in the TLS point cloud. (a) Trace lengths and (b) orientations.

2.2 Discontinuity analysis

The *pdf* of the discontinuity diameters is defined by applying a sequence of methods described in Zhang and Einstein, 2000:

First, a goodness-of-fit test (such as the Kolmogorov-Smirnov test) is used to find the *pdf* of the measured trace lengths [$f(l)$], of each discontinuity set. The most common distribution for trace lengths are the log-normal, gamma and negative exponential (Zhang and Einstein, 2000).

Next, a tunnel section is chosen and window-sampling method is used to find the unbiased mean trace lengths and standard deviations (Figure 3). Cacciari and Futai (2016) tested several window-sampling methods and found the method proposed by Wu et al. (2011) more suitable for tunnels. In this method, the unbiased mean trace length (μ) is calculated as:

$$\mu = \frac{wh(1 + R_0 - R_2)}{(1 - R_0 + R_2)(wB + hA)} \quad (1)$$

where w is the width, h is the height of a rectangular window, R_0 and R_2 are the fractions of transecting (both ends censored) and contained (both ends observable) traces. A and B are constants that depend on the discontinuity set and rock face orientations (see more details in Wu et al., 2011 and Cacciari and Futai, 2016). The standard deviation (σ) is calculated using the coefficient of variation (Zhang and Einstein, 2000), as:

$$\sigma = \mu \times cv_m \qquad cv_m = \sigma_m / l_m \quad (2)$$

Where σ_m, l_m and cv_m are the mean, standard deviations and coefficient of variation of the measured trace lengths, respectively, and can be directly obtained from the TLS discontinuity data.

The tunnel was subdivided in tree regions with a fitted rectangular sampling-window in each one of them: the roof (R), the east-wall (EW) and the west-wall (WW). Figure 3a shows a section of the tunnel with this subdivision and the trace map obtained from TLS. The walls were considered vertical sampling planes and the roof a horizontal sampling plane to simplify the application of Eq. 1. Figure 3b shows the roof of the tunnel section mapped with TLS and Figure 3c shows the trace map with the rectangular sampling window fitted to calculate μ and σ.

The unbiased trace length *pdf* $[g(l)]$ is obtained by replacing the mean and standard deviation of $[f(l)]$ by μ and σ, and assuming the same distribution form (e.g. log-normal, gamma, etc.). Finally, the discontinuity diameter *pdf* is obtained by the method proposed by Zhang and Einstein (2000), using the following equations:

$$\mu = \frac{\pi\left[(\mu_D)^2 + (\sigma_D)^2\right]}{4\mu_D} \quad (3)$$

$$\left[(\mu)^2 + (\sigma)^2\right] = \frac{2E(D^3)}{3\mu_D} \quad (4)$$

$$\frac{E(D^4)}{E(D^2)} = \frac{E(l^3)}{E(l)} \quad (5)$$

where μ_D and σ_D are the mean and standard deviation of $[g(D)]$; $E(D^n)$ and $E(l^n)$ are the n^{th} moments of $g(D)$ and $g(l)$, respectively.

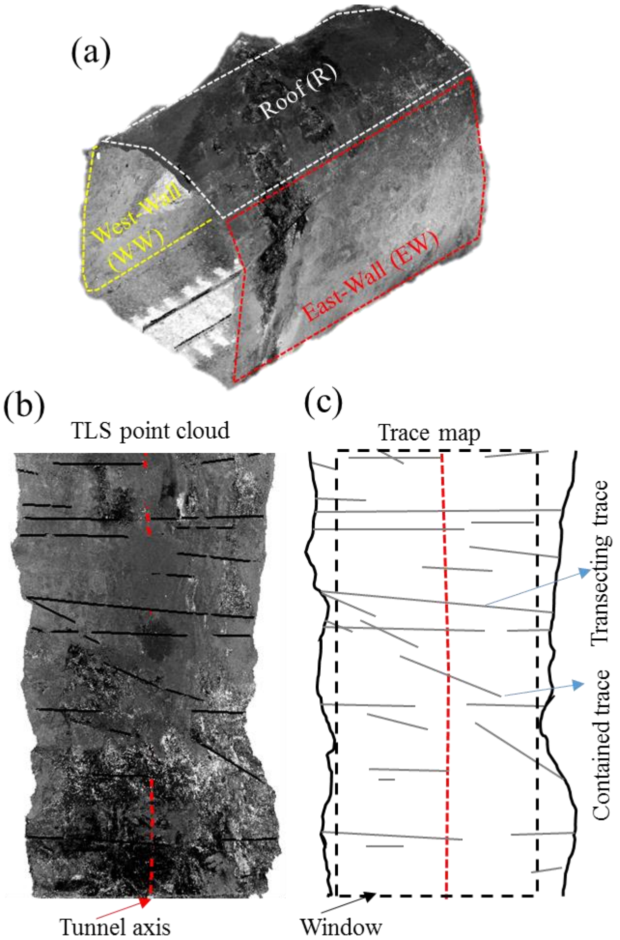

Figure 3. (a) Section of the tunnel indicating the three regions. (b) TLS mapped point cloud of the R region and (c) trace map with the rectangular sampling window.

According to Zhang and Einstein (2000), the application of Eqs. 3, 4 and 5 is an interactive procedure, consisting in:

1) Guessing the $g(D)$ distribution form (log-normal, gamma, exponential, etc.) and obtaining $E(D^3)$ as a function of μ_D and σ_D.

2) Replacing the $E(D^3)$ expression in Eq. 4 and solving Eqs, 3 and 4 to find μ_D and σ_D values (considering that μ and σ are already obtained by Eqs. 1 and 3).

3) Obtaining the expressions and calculating the 4th and 2th moments of $g(D)$ in Eq. 5 (with the guessed distribution form) and calculating de 1th and 3th moments of $g(l)$.

4) Comparing the left and right sides of Eq. 5. The closer the values, the better the distribution form adopted. Generally, the same distributions ordinarily used for trace length are tested for discontinuity diameters. However, with this method the $g(D)$ and $g(l)$ forms are not necessarily the same.

The discontinuity orientations are directional data that cannot be directly used in conventional goodness-of-fit tests. Thus, the discontinuity analysis of orientation data is simplified here by assuming different Fisher distributions for each discontinuity set. Therefore, the mean Dip/Dip Direction and the Fisher constant K (or dispersion factor) describe the orientation *pdf* of each discontinuity set.

2.3 P32 calculation from DFN generations

The volumetric discontinuity intensity (P32) is defined as the total discontinuity area per unit of rock mass volume. P32 is the best parameter to represent the discontinuity intensity because it considers both unbiased frequency and size components (Rogers et al. 2015; Haveaj et al. 2015). However, as it is impossible to sample discontinuity areas in field surveys, P32 must be estimated from 2D discontinuity samplings (trace maps) in rock outcrops.

One possible approach to estimate P32 is to use DFNs to simulate conditions similar to those observed in field. Once the *pdfs* of discontinuity diameters and orientations of each discontinuity set are known, the number of discontinuities intersecting a sampling plane (such as in Figure 3c) or a scanline can be used as the stopping criteria for disk-shape discontinuity generation in a given DFN volumetric domain. The 3DEC program uses a Poisson process to generate discontinuities in the DFN domain and computes the number of discontinuities intersecting a rectangular polygon placed inside the model, with the same dimensions as that used in TLS point cloud (Figure 3c). Once the number of intersections reaches the same value of that in TSL, the program stops the discontinuity generation and P32 is calculated as:

$$P32 = \frac{\sum_{i=1}^{N} S_i}{V} \qquad (3)$$

where N in the total number of discontinuities generated inside the model, S_i is the area of the i^{th} discontinuity and V the volume of the DFN domain. Figure 4a and 4b show an example of this process. The same model can be run several times and a mean P32 can be calculated to better represent the discontinuity distribution. Next, a new DFN is generated with the same *pdfs* of discontinuity diameters and orientations, but using the calculated P32 as the stopping criteria for discontinuity generation within the DFN domain.

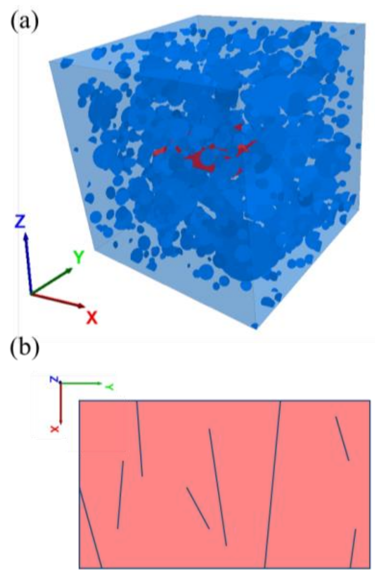

Figure 4. (a) Example of the DFN volumetric domain with the discontinuities generated and the sampling rectangular polygon placed inside the model. (b) Rectangular sampling polygon with the resulting discontinuity intersections (virtual traces).

3 EXAMPLE OF APLICATION (MONTE SECO TUNEL)

The Monte Seco tunnel is part of the Vitória-Minas Railway (VMR) and located in the State of Espirito Santo, southeastern Brazil (Figure 5). VMR is operated by Vale SA, and is responsible for transporting raw materials (mainly iron ore) from the State of Minas Gerais to the Tubarão seaport, in Vitória (State of Espirito Santo).

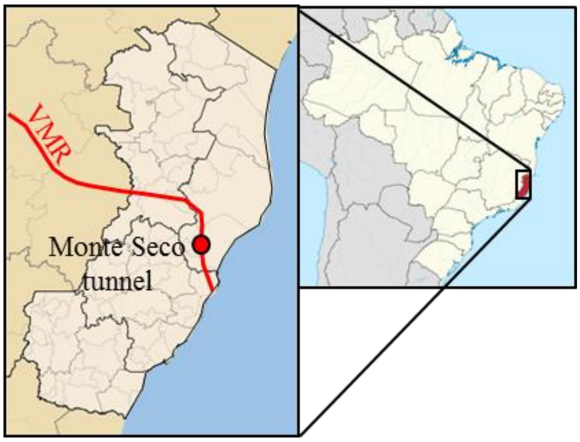

Figure 5. Geographic location of the Monte Seco tunnel.

3.1 Discontinuity analyses and P32 calculation.

The tunnel is constructed in a gneissic rock mass with four discontinuity sets identified and characterized during field inspections: Two shear fracture sets (F1 and F2); one sheet joint set (F3) and the rock foliation (Sn). The same sets were mapped in detail with TLS images. Figure 6 shows the orientation measurements in TLS images with the identifications of each of these sets and the tunnel axis.

In most cases, discontinuity trace lengths are described by lognormal, gamma or exponential distributions (Zhang and Einstein, 2000). All trace lengths from each discontinuity set (F1, F2 and F3) mapped in the TLS images of the tunnel were analyzed by Kolmogorov-Smirnov tests to find the best-fitted distribution forms. Table 1 shows the statistic results of the tested distributions (lognormal, Gamma and exponential). Figure 7 shows the best-fitted distribution (lognormal in all the cases) for each discontinuity set. Rock foliation is considered persistent in the tunnel scale, thus its traces are not analyzed here.

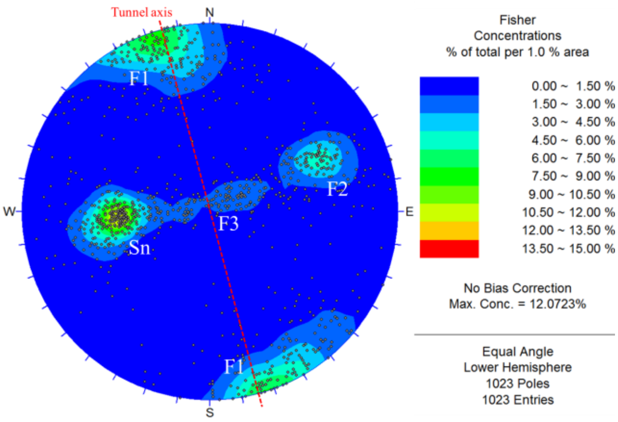

Figure 6. Stereographic plot of the discontinuity orientation (poles) measured in TLS images.

Table 1. Kolmogorov-Smirnov (K-S) statistic results (the lower the value, the better the distribution fit).

Distribution	F1	F2	F3
Lognormal	0.028	0.026	0.036
Gamma	0.094	0.071	0.140
Exponential	0.200	0.250	0.190

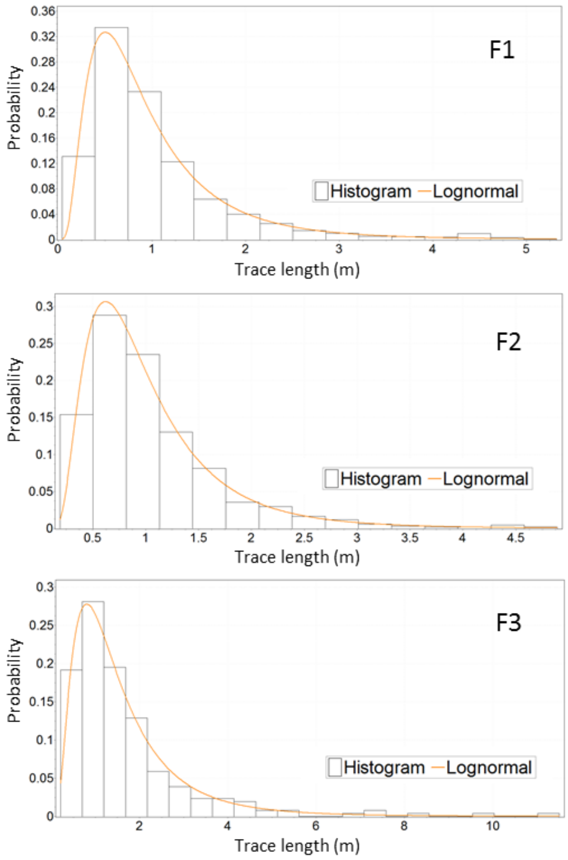

Figure 7. Lognormal distributions fitted to F1, F2 and F3 trace length data.

Following the methodology described in section 2.2, the discontinuity diameter distributions, from a particular section of the tunnel, must be found using the trace length distributions defined with the entire trace data (Figure 7). The first 324 m of the Monte Seco tunnel was fully mapped in TLS images. Thus, it is possible to select any sections in this portion to perform discontinuity analyses and to generate DFNs to create the 3DEC block model. We present an example of the complete methodology using an 8 m long section of the tunnel (Figure 8a) that was analyzed by Cacciari and Futai, 2016. The trace map of this section (obtained from the TSL mapping) is presented in detail in Figure 8b (the F3 discontinuities do not appear in this particular section of the tunnel).

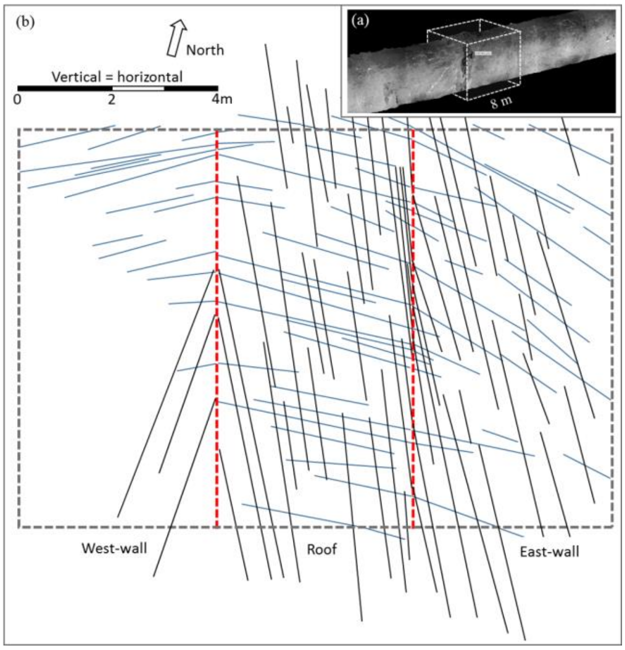

Figure 8. (a) Section chosen to apply the complete methodology. (b) Trace map of the section obtained by TLS mapping (F1 are the blue traces and F2 are the black traces) (Cacciari and Futai, 2016).

From Figure 8b, it is clear that the west-wall is much less fractured than the roof and the east-wall, which was thus not used for trace length analysis. Eqs. 1 and 2 were applied to the trace map of Figure 8b, considering the roof (horizontal) and the east-wall (vertical) as rectangular sampling windows. Table 2 summarizes the results for F1 and F2 fracture sets.

Table 2. Trace length analysis. (R) Roof window; (EW) East-wall window.

Disc. set	cv_m	μ (m)		σ (m)	
		R	EW	R	EW
F1	0.51	3.9	2.6	1.98	1.32
F2	0.50	4.9	3.2	2.45	1.60

With the results presented in Table 2, Eqs 3, 4 and 5 were applied to find the *pdfs* of discontinuity diameters of F1 and F2. The same distribution forms (lognormal, gamma and exponential) were tested by the interactive process described in section 2.2. After the definition of $g(D)$, the DFN-3DEC simulations described in section 2.3 (Figure 4) were used to obtain the P32 values for F1 and F2 sets. Ten DFN generations were generated in this process and the mean P32 was calculated. Table 3 shows the $g(D)$ results and Table 4 shows the P32 values obtained using $g(D)$, the Fisher parameters (of this specific 8 m long section) and the number of discontinuities intersecting the sampling windows (N).

Table 3. Discontinuity diameter analysis. (R) Roof window; (EW) East-wall window; (LN) lognormal *pdf*.

Disc.	Test from Eqs. 3-5		μ_D/σ_D (m)	
Set	R	EW	R	EW
F1	**LN**	LN	**4.3/1.7**	2.8/1.1
F2	LN	**LN**	5.4/2.1	**3.5/1.4**

Table 4. P32 analysis. (R) Roof window; (EW) East-wall window.

Set	Fisher parameters		N		P32 (m^{-1})	
	K	Dip/Dip.Dir.	R	EW	R	EW
F1	46	62/245	**31**	30	**1.8**	1.4
F2	21	86/159	29	**24**	2.7	**2.8**
Sn	73	53/085	-	-	-	-

The bold values in Table 3 and 4 are those used to obtain the highest P32 between the R and the EW samples, for each discontinuity set. It is worth noting the influence of the discontinuity orientation in P32 results by comparing the highest P32 values obtained from F1 and F2 sets. F1 fractures are perpendicular to the tunnel axis and sub-vertical (Figure 6), thus, the probabilities of intersection between F1 and

R (horizontal surface) or EW (vertical surface) are similar. Consequently, we expected to obtain the highest P32 with the highest values of N and μ_D. On the other hand, F2 fractures are sub-parallel to the tunnel axis and dip steeply to west (Figure 6), thus, the probability of intersection between F2 and R is higher than F2 and EW. The same differences between probabilities of intersection are reproduced in the DFN generations, when horizontal or vertical virtual sampling surfaces are inserted in the model for intersection counting (Figure 4). Therefore, for F2, the P32 value obtained from EW was the highest, even with the lower values of N and μ_D (Table 3 and 4).

3.2 DFN and block model generation.

The mean P32 values calculated are used as stopping criteria for new DFN generations, with the same $g(D)$ and Fisher distributions used to obtain them (Table 3 and 4). In this example, the rock foliation (Sn) was considered a persistent structure with a deterministic spacing $S = 0.5$ m (or frequency $\lambda = 2$ m^{-1}). The 3DEC blocks are generated by the intersection of F1, F2 and Sn discontinuities. Figure 9a shows the DFNs created around the tunnel area and 9b the resulting block model.

The discontinuity mapping (orientation and trace length measurements) is the only manual step of the present methodology. The discontinuity analyses and DFN-3DEC modelling are automated by Excel-Visual Basic subroutines associated with DFN codes written in Fish (3DEC programming language). Thus, with the TLS complete mapping of the tunnel, any other section (with different position and length) could also be modelled. Moreover, if the TLS is used during tunnel construction and the discontinuity mapping is constantly updated (for each tunnel advance) the same methodology could also be used for creating 3DEC block models.

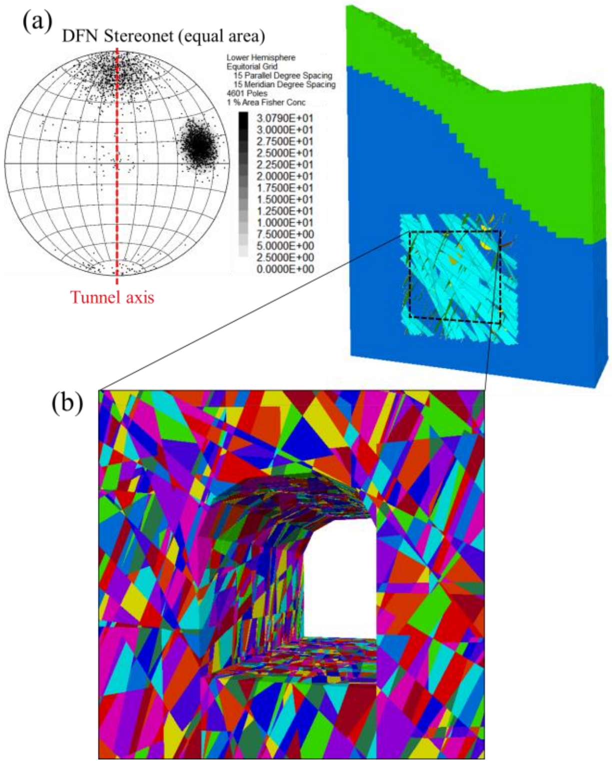

Figure 9. (a) DFNs generated around the tunnel with the stereographic plots. (b) Final 3DEC block model of the 8 m long section of the Monte Seco Tunnel.

4 CONCLUSIONS

A methodology integrating terrestrial laser scanning and discrete fracture networks was presented for tunnel modelling in fractured rock masses. The 3DEC software was used to generate DFNs and the block model of an 8 m long section of the Monte Seco tunnel.

TLS is a practical and powerful tool for discontinuity mapping in tunnels because it overcomes difficulties associated with the traditional hand-made geological mapping (Lato et al., 2010; Cacciari and Futai, 2016), allowing equal examinations of all regions of the tunnel (walls and roof). Moreover, a sophisticated window-sampling method could be applied to determine $g(D)$, but only because the detailed TLS discontinuity mapping was available.

The integration between TLS mapping; discontinuity analyses and DFN modeling was used to calculate P32, which is the most representative discontinuity intensity parameter used as stopping criteria for DFN models.

In this case, an 8 m long section of the tunnel was analyzed to exemplify the methodology proposed. However, the discontinuity analyses and DFN modeling process are both automatic processes; Thus, they can be applied to any other section of the tunnel.

ACKNOWLEDGEMENTS

The authors would like to thank the company VALE SA, FAPESP and the Brazilian National Council of Scientific and Technological Development (CNPq) for the logistical and financial support.

REFERENCES

Cacciari, P.P.; Futai, M.M. (2016) Mapping and characterization of rock discontinuities in a tunnel using 3D terrestrial laser scanning. *Bull Eng Geol Environ*, Vol. 75, p. 223–237.

Havaej, M.; Coggan, J.; Stead, D. and Elmo, D. (2015) A combined remote sensing–numerical modelling approach to the stability analysis of Delabole slate quarry, Cornwall, UK. *Rock Mech Rock Eng*, Vol 49, p. 1227-1245.

Lato, M.J.; Diederichs, M.S. and Hutchinson, D.J. (2010) Bias correction for view-limited lidar scanning of rock outcrops structural characterization. *Rock Mech Rock Eng*, Vol. 43, p. 615-628.

Rogers, S.; Elmo, D.; Webb, G. and Catalan, A. (2015) Volumetric fracture intensity measurement for improved rock mass characterization and fragmentation assessment in block caving operations, *Rock Mech Rock Eng*, Vol. 48, p. 633–649.

Wu, Q.; Kulatilake, P.H.S.W. and Tang, H. (2011). Comparison of rock discontinuity mean trace length and density estimation methods using discontinuity data from an outcrop in Wenchuan area, China, *Comput Geotech*., Vol. 38, p. 258-268.

Zhang, L. and Einstein, H.H. (2000) Estimating the intensity of rock discontinuities, *Int J Rock Mech Min Sci*, Vol. 37, p. 819-837.